

# Cellulose nanocrystals/polyaniline particles' dispersion in polypropylene nanocomposites

Lilia BENCHIKH<sup>1\*</sup>; Yazid AITFERHAT<sup>2</sup>; Maya KEBAILI<sup>2</sup>, Ilyes ABACHA<sup>2</sup>, Melia GUESSOUM<sup>3</sup>, Abdelhafid MERZOUKI<sup>3</sup>, Yves GROHENS<sup>4</sup>

<sup>1</sup>Centre de Recherche en Technologies Agroalimentaires. Route de Targa Ouzemmour, Campus Universitaire, Bejaia, 06000. Algeria

<sup>2</sup>Centre de recherche en mécanique, Campus Chaab Erssas, Université les frères Mentouri 1, Constantine 25021, Algérie

<sup>3</sup>Laboratoire Physico-Chimie des hauts polymères, université Ferhat Abbas, Setif 1, Setif 19000, Algérie

<sup>4</sup>Institut de Recherche Dupuy de Lôme, UMR CNRS 6027, Université de Bretagne Sud, Lorient, France

\*Corresponding author email: [lilia.benchikh@gmail.com](mailto:lilia.benchikh@gmail.com)

Received: 15 November, 2023; Accepted: 16 December, 2023; Published: 22 January, 2024

## Abstract

*Sustainable development and biomass valorization are a primary means of reducing the non-renewable resources consumption and an opportunity to exploit the agricultural and forestry sectors where biomass as a renewable resource will play an important role. Cellulose is the most abundant bio-renewable material and its unique structure generates nanoparticles known as cellulose nanocrystals (CNC). Cellulose nanomaterials show a great promise for various applications therefore with a relatively low loading level, significant improvements on mechanical properties of nanocomposites could be obtained, but CNCs have a strong tendency to agglomerate and its hydrophilic characteristic leads to interfacial incompatibility with non-polar polymer matrices.*

*In this work, polyaniline (PANI) is used as a support for Cellulose nanocrystals dispersion on Polypropylene (PP) matrix. Cellulose nanocrystals were obtained according to an experimental protocol at several stages and Polyaniline was deposited on CNC's surface during polyaniline synthesis in CNC's suspension. The obtained CNC/PANI nanoparticles were incorporated into the polypropylene matrix by melting compounding technique. Polypropylene nanocomposites and PANI/CNC particles were characterized with different techniques: FTIR, AFM, electrical conductivity and mechanical properties to study and assess how polyaniline and CNC affect microstructure, morphology and electrical properties of PP. Characterization technique showed that PANI was successfully synthesized on CNC's surface and PANI/CNC material is a semiconductor. The enhanced mechanical properties of PP/PANI-CNC nanocomposites indicates a good dispersion of CNCs particles on PP matrix.*

**Keywords:** Cellulose nanocrystals, CNC, Polyaniline, Polypropylene, Nanocomposites

## I. Introduction

In the era of sustainable development, it is important to produce high-performance, value-added materials from abundant renewable resources and cellulose from photosynthesis, is the most abundant polymer on earth [1].

Cellulose can be transformed into micro- and nanoscale materials by various chemical, enzymatic and mechanical treatments and depending on their morphology and properties; it consists of cellulose nanocrystals (CNC), nanofibers cellulose (CNF) and bacterial cellulose (BC) [2,3]. Nanocellulose enjoys specific properties such as high aspect ratio, high specific modulus, relatively good surface

reactivity and non-toxicity, as well as being readily available, renewable and biodegradable [4]. The variety of dimensions, morphologies, degrees of crystallinity depend on the source of cellulosic material and the conditions under which the preparation is carried out [5]. Nanocellulose is easily accessible nanofiller for the fabrication of novel nanocomposites [6].

Thermoplastics, particularly Polypropylene (PP), are consumed in large quantities. PP is widely used in industry due to its ease of processing, low cost and good overall properties [7,8]. However, PP is largely limited by insufficient strength and poor thermal properties [9].

Therefore, PP is usually loaded by particles and fibers to obtain composites with better properties [10,11].

Polyaniline (PANI) is one of the most common conductive polymers due to its high electrical conductivity, high environmental stability in addition to relatively low cost [12]. Potential uses of polymer/PANI blends are in the areas of electronic components and coatings; and PP/PANI composites can be used as membranes [13,14]. Also, Hybridization of PANI with other materials has been exploited to improve PANI's properties [15].

CNCs have been usually applied as nanoreinforcement in polyolefin, polyester, rubber, polyurethane (WPU), epoxy resins and natural polymers, etc.; and processable nanocomposites of PANI and both CNF and CNC, have successfully been made [16-18]. PANI lignocellulose composites are used as absorbents to remove commonly used dyes, which are non-biodegradable and toxic to humans and environment [17,18].

On the other hand, nonpolar matrices have low interfacial compatibility with polar nanocellulose attributed to the hydrogen bonds on CNCs surface forming agglomerations and requires various methods of modifying fillers or matrices to promote interactions between filler and matrix [19-21]; Among these techniques of modification, casting/evaporation nanocomposites preparation is predominant. In-situ polymerization has also been reported in nanocomposites preparation with polyolefin matrices [22]. This method consists of polymerizing the reactive monomers with the nanoparticles.

In this present work, CNC/PANI nanocomposites were successfully developed by in situ polymerization of aniline in a CNC suspension with the main objective of covering the CNCs surface with PANI in order to reduce the hydrogen bonds between CNCs particles and allow optimal dispersion of PANI-CNC in PP matrix. PP/PANI composites with different PANI-CNC contents (0, 0.5, 1, 2 and 3 wt%) and compatibilized with PP-g-MA were prepared by hot mechanical mixing. The obtained nanocomposite materials were characterized by different structural, mechanical and rheological techniques. CNC-PANI's dispersion state in the PP matrix was also observed by AFM.

## II. Material and methods

CNCs were extracted from *El Diss* (*Ampelodesmos mauritanicus*). CNCs nanocrystals preparation method and characterization details were reported earlier by Benchikh and al. [23]. The used polypropylene is "HG385MO" produced by "Borouge", with a density of 0.91 g/cm<sup>3</sup> and a melt flow index of 25g/10min (at 230° C and under 2.16 kg). The PP-g-MA used is polybond 3200, a polypropylene grafted with maleic anhydride, commercialized by Cromptan

Unioroyal Chemical with a density of 0.91 g/cm<sup>3</sup> and a melt flow index of 11.5g/10min. The reagents used for PANI preparation are : Hydrochloride acid (HCL), aniline, Ammonium persulfate (APS), purchased from CARLO ERBA (Cornaredo, Milan, Italia) and Biochem Chemical Pharma (Montreal, Quebec, Canada).

CNC/PANI nanocomposites were prepared according to the procedure described as follows: An aniline solution was first prepared by dissolving aniline (0.2 mol /l) in concentrated HCl (0.1 M, 37 wt %), and then it was mixed with a 1% CNC suspension to obtain 1L of an homogeneous reaction mixture dispersion (dispersed in an ultrasound bath for 120 min). The obtained aqueous dispersion was put in a vial at low temperature water bath (5°C) under a constant stirring, 0.2 mol/l of APS was added drop by drop during 1h. After polymerization at 5°C for 1h, a dark green suspension was formed. Finally, the suspension was washed several times.

PP/PANI nanocomposite samples were prepared by the hot pressing method. PP/PANI mixtures were obtained by blending PP matrix with PANI-CNC powder in different weight percentages (0, 0.5, 1, 2 and 3% wt) in a Brabender (GmbH & Co.KG, Model 819952, 2010, Germany), at 200 °C for 8 minutes.

### II.1. Characterization

#### A. Fourier transform infrared spectroscopy (FTIR spectroscopy)

To investigate structural modifications after adding PANI-CNC mixture to PP, the obtained PP/PANI-CNC nanocomposites were characterized by FTIR spectroscopy. The samples were analyzed using a Perkin-Elmer (L1600400 Spectrum TWO DTGS) spectrometer, in transmittance mode (4000 cm<sup>-1</sup>-400 cm<sup>-1</sup>, 2 cm<sup>-1</sup>).

#### B. Atomic force microscopy (AFM)

Atomic force microscopy images were obtained on the different samples using an AFM microscope (contact mode, a tip of 2 Nm<sup>-1</sup>) and physical characteristics of the observed surfaces from 3-D images were quantified by measuring their roughness on a scanning surface of 10µm×10µm with a dimension of 1552×1254 pixels.

#### C. Conductivity analysis

For measuring PANI-CNC conductivity, a pellet of (PANI-CNC) is prepared, and using a multimeter, a transverse resistance is measured and converted into volume resistivity. For PP/PANI-CNC nanocomposites, electrical conductivity measurements were carried out using the Van der Pauw technique.

#### D. Melt flow index

The Melt Flow Index (MFI) is a static method widely used in industry to determine fluidity of a polymer. To carry out this analysis, PP/PANI-CNC samples were subjected to the NF EN ISO 113 standard.

### E. Mechanical tests

Tensile properties were evaluated using MTS Landmark® (MTS Systems Corporation (USA)) universal testing machine. Samples were prepared according to ASTM-D 638 and tested at a drawing speed of 5 mm/min. Izod impact strength of nanocomposites was measured by assessing samples of dimensions (62×13×3) mm<sup>3</sup> using a Ceast Resil Impact instrument equipped with a hammer of 1.8 kg delivering an impact energy of 7.5 kJ.

## III. Results and discussion

### A. Structural characterization

FTIR spectra of PANI-CNC and PP/PANI-CNC nanocomposites are shown in Figure 1.

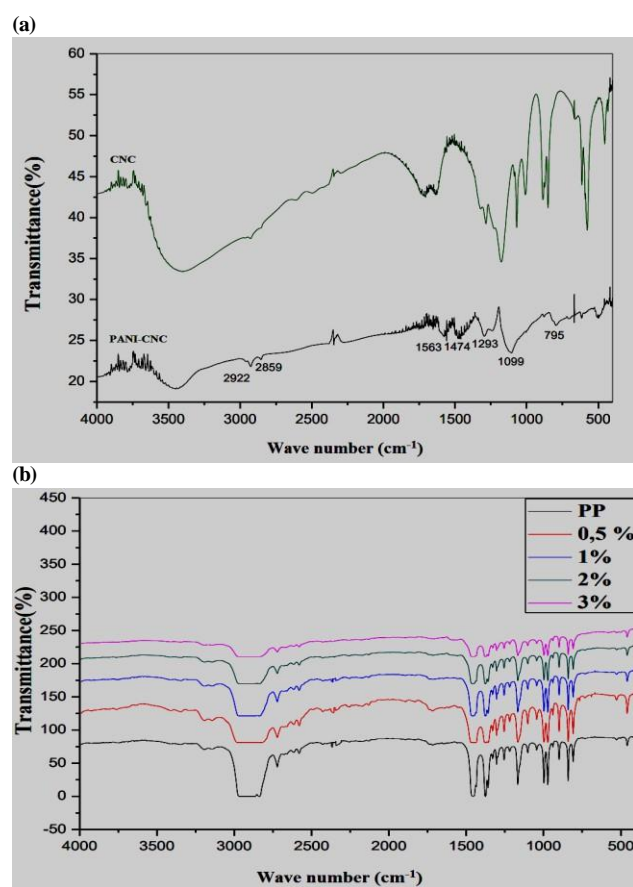


Figure 1. FTIR spectra of : (a) CNC-PANI particles, (b) PP/CNC-PANI Nanocomposites

The peaks of 1563 and 1474 cm<sup>-1</sup> came from the elongation vibration of N = Q = N and N-B-N structures, respectively (B and Q represent the fractions benzenoids and quinoids in PANI chains) and confirm that the structures are doped. The peaks at 1293 and 1140 cm<sup>-1</sup> are assigned to C-N elongation vibration and the in-plane aromatic C-H bending, respectively. The peak corresponding to C-H band out-of-plane bending vibration of the para-disubstituted benzene ring appears at 795 cm<sup>-1</sup> [24-26]. The peak at 1099 cm<sup>-1</sup> is

linked to NH<sup>+</sup> interactions with SO<sup>3-</sup> [27]. These results conclude that PANI was successfully formed on the surface of cellulose nanocrystals (CNC) during in-situ polymerization.

Figure 1 (b), presents the FTIR spectra recorded on the developed nanocomposites.

From FTIR spectra, it can be deduce that the obtained nanocomposites has the same characteristic peaks of PP. However, in PP/PANI-CNC at 3%, a new band at 3346 cm<sup>-1</sup> is appeared corresponding to the CNC hydroxyl groups elongation and a band at 1561 cm<sup>-1</sup> corresponding to quinoid groups elongation of PANI structure [28].

### B. Morphological characterization

AFM images of PANI-CNC composites (figure 2) show a rough heterogeneous surface, with dispersed aggregates. The presence of these grains in large quantities is explained by a large quantity of polyaniline, equivalent to two times the quantity of cellulose particles. These results indicate a massive deposition of PANI's particles on CNCs particles or on CNC aggregates.

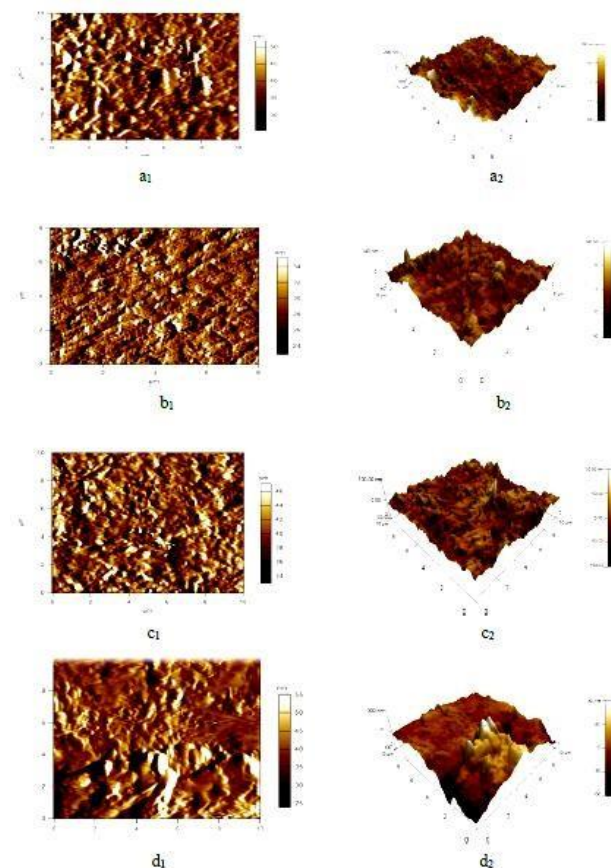


Figure 2. Image AFM of: (a<sub>1</sub>, a<sub>2</sub>) PANI-CNC, (b<sub>1</sub>, b<sub>2</sub>) PP, (c<sub>1</sub>, c<sub>2</sub>) PP/PANI-CNC 1%, (d<sub>1</sub>, d<sub>2</sub>) PP/PANI-CNC 3%

Surfaces structure evolution (topography) of pure PP and nanocomposites (1 and 3%) are irregular, covered with grains of lateral dimensions and height between 24-34/70-140 nm, 34-36/50-100 nm and 25-55/150 nm to 300 nm for PP, PP/PANI-CNC 1% and PP/PANI-CNC 3%, respectively.

PP/PANI-CNC 1% surface is relatively smooth compared to those of pure PP and PP+3%. In table 1, we have reported the roughness values noted on the materials. PP/PANI-CNC 1% shows a decrease in value of root mean square (RMS) roughness. Reduction of surface roughness can be attributed to a reduction in overall size therefore a good dispersion of filler at low concentration unlike PP at 3% where the roughness increased and can be explained by aggregates formation on the surface.

**Table 1.** Roughness values of PANI-CNC particles and PP/PANI-CNC nanocomposites

Samples	PANI-CNC	pp	PP+1%	PP+3%
Surface Roughness Measurement (nm)	35	19	16	66

### C. Electrochromic Properties

PANI-CNC in powder form, is compressed to obtain a pellet of 13.18 mm in diameter and 4.65 mm in thickness. Transverse resistance is measured and volume resistivity is calculating as follow:

$$\rho = (R \cdot \pi \cdot r^2) / e$$

$$R = 0.17 \Omega, r = 1.318 \text{ cm}, e = 0.465 \text{ cm}$$

$$\rho = 1.99 \Omega \cdot \text{cm}$$

$$\sigma = 1/\rho = 0.50 \Omega^{-1} \text{cm}^{-1}$$

The measured conductivity of (PANI-CNC) corresponds to a high range of semiconductors ( $10^{-4} \text{ S/cm} < \sigma$  semiconductor  $< 1 \text{ S/cm}$ ), demonstrating a synthesis of a PANI/CNC composite with electronic properties improved.

According to FTIR characterization, PANI-CNC synthesis by an In-situ process leads to efficient interactions between PANI quinoid ring and CNCs and facilitate the charge transfer processes between the two components [29].

On the other hand, when PANI-CNC particles is used as reinforcement in PP matrix at 0.5% and 1%, it is observed that the conductivity is almost the even. For PP/PANI-CNC 3%wt, where there is a fairly significant conductivity reduction, this has been attributed to polyaniline agglomeration tendency at high rates of loads. Conductive properties of these composites depend on the molecular organization of the conductive aggregates in relation to the polymer matrix and the geometry of the conductive charge, as well as the charge-charge interaction [26]. These results are in agreement with the morphological properties studied by AFM.

**Table 2.** Conductivity value of PP/PANI-CNC nanocomposites

Samples	Conductivity ( $10^{-18} \text{ S/cm}$ )
PP/PANI-CNC 0.5%	2.11
PP/PANI-CNC 1%	2.01
PP/PANI-CNC 2%	2.32
PP/PANI-CNC 3%	1.63

### D. Melt flow index analysis

Fluidity index evolution as a function of load rate is shown in Figure 3.

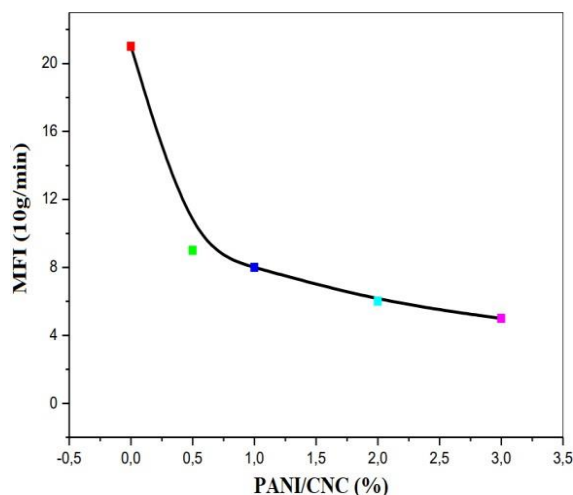
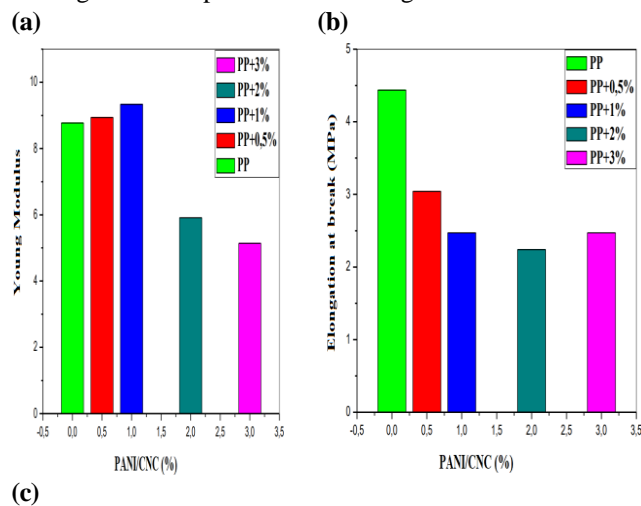


**Figure 3.** Fluidity index evolution as a function of PANI-CNC loading rate

By analyzing the obtained results, it is clear that PP's MFI (MFI= 21, more fluid) is very high compared to PP/PANI-CNC nanocomposite materials. The index fluidity decreases as a function of charge rate, molar mass (MW) increases by particles or aggregates presence of PANI-CNC. Fluidity decreases rapidly at a low rate (0.5%) then gradually, from this concentration. These results indicate that at a low rate, PANI-CNC particles are well dispersed and however, present obstacles to the flow at high loading rates [30].

### E. Mechanical characterization:

Variations in mechanical properties (Young modulus (E), elongation at break and tensile strength at break) of PP/PANI-CNC nanocomposites as a function of PANI-CNC loading rate are represented in the Figures 4.



(c)

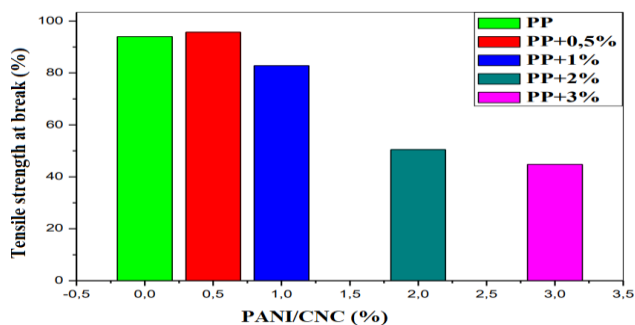


**Figure 4.** Tensile properties of PP/PANI-CNC nanocomposites: (a) Young's modulus, (b) Elongation at break, (c) Tensile strength at break

The above figures reveal that adding PANI-CNC particles increase slightly the Young modulus from 7.96 GP for pure PP to an Emax of 9.33 GP for PP at 1% loading rate.

With the addition of 0.5% by weight of PANI-CNC, nanocomposite tensile strength improved from 94 MPa for pure PP to 95.7 MPa, with a simultaneous decrease in elongation at break from 4.43% to 3.04%.

When CNC content exceeds 0.5% by weight, tensile strength and elongation at break gradually decreases while the Young's modulus has greatly increased (PP-PANI-CNC 1%). When PANI-CNC content exceeds 1% by weight, tensile strength, elongation at break and Young's modulus decrease gradually while with 3% of PANI-CNC, there is an increase in elongation at the break.

Composites mechanical properties are profoundly influenced by their composition and morphology [26], Fraysse et al [31], who carried out thermomechanical studies on PMMA/PANI composites and reported that PMMA mechanical behaviors is not modified with PANI addition for percentages of up to 0.5% by weight, while a sudden change is recorded above 1% concentration of PANI.

It has been reported that PANI addition to conventional polymers above the percolation threshold don't alters their mechanical properties because the conductive phase is dispersed in the form of separate islands in the continuous polymer matrix and it does not have a significant influence on composite macroscopic properties, therefore, while for CNC rates above the percolation threshold, the crystal structure of the polymer matrix alters and mechanical properties decrease [26,32].

These results indicate that a concentration at 0.5 and 1% is an adequate concentration for optimal distribution of PANI/CNC particles, since it has an improvement in the Young modulus and a better toughness by reducing elongation at break. Maleated coupling agents proved their efficiency in improving interfacial bonding between CNC's hydroxyl groups and hydrophobic polymers as PP [33]. This improvement confirms that PP-g-MA contributed in developing an interconnected structure from PP matrix and CNCs which are not covered by PANI through the reaction of MA groups and CNC's hydroxyls groups and anchoring of

the PP compatibilizer chains into the PP phase leading to an efficient stress transfer between these components. Accordingly, it is reported that improvement of uniaxial traction properties is due to the homogeneous distribution of CNCs in PP matrix and bonds formation with the compatibilizer [34,35].

Izod impact tests were carried out as a function of PANI-CNC mass percentage and represented in Figure 5.

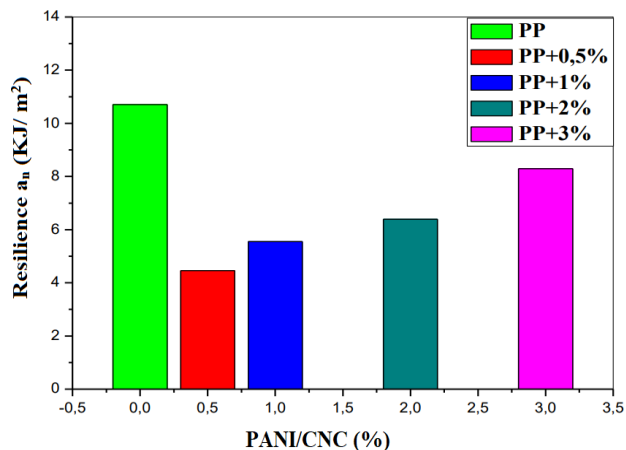


**Figure 5.** Variations of impact strength for PP/PANI-CNC nanocomposites versus PANI-CNC content

Figure 5 shows the impact resistance evolution; we observed a drop in PP resilience with a load rate at 0.5% of PANI-CNC which agree with the tensile results. Above this concentration, a slight improvement in impact resistance is observed.

## Conclusion

In the present paper, cellulose nanocrystals CNC were incorporated into a polypropylene PP matrix for the development of improved nanocomposites. For this, Polyaniline was synthesized by oxidative polymerization in the presence of CNCs in suspension as support for CNCs optimal distribution. PANI-CNC blend was incorporated into PP matrix. PP-grafted maleic anhydride was used to develop interactions between non-PANI-related CNCs with PP.

Characterization by measuring conductivity by a multimeter confirmed the conductive nature of the PANI/CNC composites and therefore of the synthesized Polyaniline. Conductivity measurement is in the high range of semiconductors.

FTIR characterization shows that PANI was polymerized on cellulose nanocrystals surface illustrated by appearance of CNC's and PANI characteristic peaks in the infrared spectrum of PANI/CNC composites. AFM results also showed that PANI covered the CNCs.

PP/PANI-CNC nanocomposites development was carried out by melt mixing. Mechanical characterization of composites based on PP loaded with PANI/CNC particles shows an improvement in mechanical performance of these

nanocomposites, this improvement is due to the particles good dispersion within the matrix, especially at low loading rates 0.5 to 1%.

We observe a drop in resilience with a CNC-PANI loading rate of 0.5%, which is in agreement with tensile results, a progressive improvement up to 3%, this is due to the particles morphology, their dispersion, their orientation and interactions.

Electrical characterization carried out by the four-point method on the composite materials shows that the produced films have a low conductivity and the highest value is noted on the nanocomposites with 2% PANI-CNC. However, the resulting composites did not achieve the conduction levels shown by PANI-CNC blend alone.

At high PANI-CNC loading rates, it tend to agglomerate into aggregates.

#### **Acknowledgment**

The author(s) received no financial support for the research, authorship, and/or publication of this article.

#### **Conflict and interest**

The author(s) declared no potential conflicts of interest with respect to the research, authorship, and/or publication of this article.

#### **References.**

- [1] J. He, N. Li, K. Bian, G. Piao. Optically active polyaniline film based on cellulose nanocrystal. *Carbohydrate Polymers* 208, 398-403, 2019
- [2] K. Jedvert, T. Heinze. Cellulose modification and shaping – a review. *Journal of Polymer Engineering* 37, pp 1-16, 2017.
- [3] A. Dufresne. Cellulose nanomaterial reinforced polymer nanocomposites. *Current Opinion in Colloid & Interface Science* 29, 1–8, 2017.
- [4] H. An, W. Ying, X. Wang, L. Na, L. Zheng. The preparation of PANI/CA composite electrode material for supercapacitors and its electrochemical performance. *Journal of Solid State Electrochemistry* 14, 651-657, 2010.
- [5] Y. Habibi, L.A. Lucia, O.J. Rojas. Cellulose Nanocrystals: Chemistry, Self-Assembly, and Applications. *Chemical Reviews* 110, 3479-3500, 2010.
- [6] M. Kılıç, Ü. Alkan, Y. Karabul, H. B. Yamak, O. İçelli. The Effects of PANI Concentration on the Mechanical Properties of PP/PANI Composites. *Afyon Kocatepe University Journal of Science and Engineering* 18, 426-433, 2018.
- [7] D. Byelov, P. Panine, W. H. de Jeu. Shear-Induced Smectic Order in Isotactic Polypropylene Revisited. *Macromolecules* 40, 288–289, 2007.
- [8] J.S. Kim, D.H. Kim. Compatibilizing effects of maleic anhydride-grafted-polypropylene (PP) on long Carbon fiber-reinforced PP composites. *Journal of Thermoplastic Composite Materials* 28, 1599–1611, 2015.
- [9] J.Z. Liang, T.Y. Zhou, S.Y. Zou. Non-isothermal crystallization properties of polypropylene composites filled with multi-walled carbon nanotubes. *Polymer Testing* 55, 184–189, 2016.
- [10] X. Wang, J. Liu, S. Zhang, D. Chimin. Flexible conductive polyaniline-silica/polypropylene composite membrane. *Synthetic Metals* 162, 1459–1463, 2012.
- [11] A. Ameli, P.U. Jung, C.B. Park. Electrical properties and electromagnetic interference shielding effectiveness of polypropylene/carbon fiber composite foams. *Carbon* 60, 379–391, 2013.
- [12] Zh. A. Boeva, V.G. Sergeyev. Polyaniline: Synthesis, Properties, and Application. *Polymer Science Series C* 56, 144–153, 2014.
- [13] S.I. Abd Razak, W.A.W. Abdul Rahman, S. Hashim, M.Y. Yahya. Polyaniline and their Conductive Polymer Blends: A Short Review. *Malaysian Journal of Fundamental and Applied Sciences* 9, 74–80, 2013.
- [14] S. Piletsky, E. Piletska, A. Bossi, N. Turner, A. Turner. Surface Functionalization of Porous Polypropylene Membranes with Polyaniline for Protein Immobilization. *Biotechnology and Bioengineering* 82, 86-92, 2003.
- [15] S. Zhang, G. Sun, Y. He, R. Fu, Y. Gu, Sh. Chen. Preparation, Characterization, and Electrochromic Properties of Nanocellulose-Based Polyaniline Nanocomposite Films. *ACS Appl. Mater. Interfaces* 9, 16426–16434, 2017.
- [16] A. Chiolerio, S. Bocchini, M. Crepaldi, K. Bejtka, C. F. Pirri. Bridging Electrochemical and Electron Devices: Fast Resistive Switching Based on Polyaniline from One Pot Synthesis Using FeCl<sub>3</sub> as Oxidant and Co-Doping Agent. *Synthetic Materials* 229, 72-81, 2017.
- [17] N. D. Luong, J. T. Korhonen, A.J. Soininen, J. Ruokolainen, L.S. Johansson, J. Seppälä. Processable Polyaniline Suspensions Through in Situ Polymerization onto Nanocellulose. *European Polymer Journal* 49, 335-344, 2013.
- [18] W. He, J. Tian, H. Jin, Y. Li. Characterization and Properties of Cellulose Nanofiber/Polyaniline Film Composites Synthesized through in Situ Polymerization. *Bioresources* 11, 8535- 8547, 2016.
- [19] A.L. Goffin, J.M. Raquez, E. Duquesne, G. Siqueira, Y. Habibi, A. Dufresne, Ph. Dubois. From interfacial ring opening polymerization to melt processing of cellulose nanowhisker-filled polylactide-based nanocomposites. *Biomacromolecules* 12, 2456–2465, 2011.

- [20] A.L. Goffin, J.M. Raquez, E. Duquesne G. Siqueira, Y. Habibi, A. Dufresne, Ph. Dubois. Poly( $\epsilon$ -caprolactone) based nanocomposites reinforced by surface-grafted cellulose nanowhiskers via extrusion processing: morphology, rheology, and thermo-mechanical properties. *Polymer* 52, 1532–1538, 2011.
- [21] J.M. Raquez, Y. Murena, A.L. Goffin, Y. Habibi, B. Ruelle, F. DeBuyl, Ph. Dubois. Surface-modification of cellulose nanowhiskers and their use as nanoreinforcers into polylactide: a sustainably-integrated approach. *Composites Science and Technology* 72, 544–549, 2012.
- [22] X. Ma, Y. Wang, Y. Shen, J. Huang, A. Dufresne. Current Status of Nanocellulose-Based Nanocomposites. In Jin Huang, Alain Dufresne, and Ning Lin (Eds), *Nanocellulose*, Inc, Wiley-VCH Verlag GmbH & Co. KGaA, 155–200, 2019.
- [23] L. Benchikh, A. Merzouki, Y. Grohens, M. Guessoum, I. Pillin. Characterization of cellulose nanocrystals extracted from El Diss and El Retma local plants and their dispersion in poly(vinyl alcohol-co-ethylene) matrix in the presence of borax. *Polymers and Polymer Composites* 29, 218-230, 2021.
- [24] D. Zhang, L. Zhang, B. Wang and G. Piao. Nanocomposites of Polyaniline and Cellulose Nanocrystals Prepared in Lyotropic Chiral Nematic Liquid Crystals. *Journal of Materials*, 1-6, 2013.
- [25] S. Zhang, G. Sun, Y. He, R. Fu, Y. Gu and S. Chen. Preparation, Characterization, and Electrochromic Properties of Nanocellulose-Based Polyaniline Nanocomposite Films. *ACS Appl. Mater. Interfaces* 19, 16426-16434, 2017.
- [26] U.M. Casado, M.I. Aranguren, N.E. Marcovich. Preparation and characterization of conductive nanostructured particles based on polyaniline and cellulose nanofibers. *Ultrasonics Sonochemistry* 21, 1641-1648, 2014.
- [27] J. A. Marins, B. G. Soares, K. Dahmouche, S. J. L. Ribeiro, H. Barud, D. Bonemer, Structure and properties of conducting bacterial cellulose-polyaniline nanocomposites. *Cellulose* 18, 1285-1294, 2011.
- [28] L. Benchikh, Y. Aitferhat, M. Kebaili, H. Chorfi, I. Abacha, M. Guessoum, A. Merzougui, H. M. Benia, Y. Grohens. Acetylation of cellulose nanocrystals extracted from cotton for drilling fluid application: structural and thermal characterization. *International Journal of Nanoscience* 22, 2023.
- [29] M. Cochet, W. K. Maser, A. M. Benito, M. A. Callejas, M. T. Martínez, J. M. Benoit, J. Schreiber, O. Chauvet. Synthesis of a new polyaniline/nanotube composite: “in-situ” polymerisation and charge transfer through site-selective interaction. *Royal Society of Chemistry* 16, 1450-1451, 2001.
- [30] L. Benchikh, A. Merzouki, Y. Grohens, I. Pellin. Extruded poly(ethylene-co-vinyl alcohol) composite films reinforced with cellulosic fibers isolated from two local abundant plants. *Journal of Fundamental and Applied Sciences* 12, 49-72, 2019.
- [31] J. Fraysse, J. Planès, A. Dufresne, A. Guermache. Thermo mechanical Studies of Poly (aniline)/Poly (methyl methacrylate) Blends: Relationship with Conducting Properties. *Macromolécules* 34, 8143 - 8148, 2001.
- [32] J. Huang, P.R. Chang, Y.Chen, S.Gao and J. Lia. Fully Green Cellulose Nanocomposites. In H. Kargarzadeh, I. Ahmad, S. Thomas, and A. Dufresne (Eds), *Handbook of Nanocellulose and Cellulose Nanocomposites*, Wiley-VCH Verlag GmbH & Co, Inc, Germany; pp 918, 2017.
- [33] M. E. González-López, J. R. Robledo-Ortíz, R. Manríquez-González, J. A. Silva-Guzmán, A. A. Pérez-Fonseca. Polylactic acid functionalization with maleic anhydride and its use as coupling agent in natural fiber biocomposites: a review. *Composite Interfaces* 25, 1–24, 2018.
- [34] Z. Kassab, F. Aziz, H. Hannache, H.B. Youcef, M. El Achaby. Improved mechanical properties of k-carrageenan-based nanocomposite films reinforced with cellulose nanocrystals. *International Journal of Biological Macromolecules* 123, 1248-1256, 2018.
- [35] M. Achaby, Z. Kassab, A. Barakat, A. Aboulkas. Alfa fibers as viable sustainable source for cellulose nanocrystals extraction: Application for improving the tensile properties of biopolymer nanocomposite films. *Industrial Crops and Products* 112, 499-510, 2018.